The link between clay composition and the location of a geothermal system reservoir: a case of Rantau Dedap geothermal system

Kartika P. Savitri[1,2], Christoph Hecker[1], Fiorenza Deon[1], Mauliate A.H. Sihotang[3], Freek D. van der Meer[1], Herwin Azis[3]

[1] University of Twente, Faculty of Geo-information Science and Earth Observation (ITC), Enschede, the Netherlands

[2] University of Gadjah Mada, Faculty of Engineering, Department of Geological Engineering, Yogyakarta, Indonesia

[3] PT Supreme Energy Rantau Dedap, Jakarta, Indonesia

k.p.savitri@utwente.nl

Keywords: clay minerals, XRD, infrared spectroscopy, infrared imaging spectroscopy, reservoir, hydrothermal alteration, geology, geothermal

ABSTRACT

The geothermal industry has extensively used clay minerals as indicators for changes in temperature and circulation zones in geothermal systems. The latter includes marking the extent of the reservoir section and permeability within the system. Methylene blue (MeB) stain test value and geophysical resistivity data are often the primary tools to locate the reservoir section, especially in the early geothermal exploration stage. The reservoir section is marked by delineating the encompassing clay cap based on the distribution of smectite clay, indicated by a higher MeB value and the existence of a conductive layer. In this paper, we compare the MeB and magnetotelluric (MT) resistivity values with the clay minerals content of rocks, among others, smectite. Whereas the identification of clay mineral composition has typically relied on X-ray diffraction (XRD), we used three analytical methods (i.e. non-imaging infrared spectroscopy (IRS), infrared imaging spectroscopy (IRIS), and XRD). Our research used extracted clay fraction of ground cuttings and the original cuttings taken from the Rantau Dedap geothermal system in Sumatra (Indonesia). The IRS and XRD analyses were done on the same clay fraction, first on air-dried fraction and then on the ethylene glycol treated fraction, while IRIS was done on the original cuttings. The clay minerals identification from the three analytical methods showed similar results. Then, the comparison with MeB test results showed that smectite has the most effect on this test results, followed by mixtures of smectite-chlorite and smectite-illite. The MT resistivity value is a function of clay mineral types and lithology. Different types of clay are associated with varying resistivity ranges; from lowest to highest are smectite, mixtures between smectite and chlorite/illite, kandites, illite and chlorite. Comparing clay composition and MeB and MT resistivity data has given a better understanding of the reservoir location in Rantau Dedap.

1. INTRODUCTION

Identifying the location of the reservoir is essential for the development of geothermal industry. Some of the main tools used in geothermal exploration are MeB stain test and MT resistivity survey. The MeB test is a titration test which can detect the amount of smectite based on the volume of MeB liquid needed to change the colour of the rock solution (Rosenberg, 2008). On the other hand, the resistivity of formation in geothermal systems is affected by several factors: (1) type of rocks and their properties, including porosity and mineral composition; (2) water saturation and fluid resistivity; and (3) temperature (Ussher et al., 2000). However, previous works indicated that temperature and fluid salinity has less effect on the resistivity variation. Both methods are suitable for locating the smectite-rich clay cap encompassing the system's reservoir. Still, the latter method can also indicate the permeability and reservoir structure of the geothermal systems in more detail based on the conductivity-resistivity configuration calculated by the model. This configuration also represents the changes in clay composition within the system.

To date, the application of non-imaging infrared spectroscopy to identify minerals and, especially, clay composition in geothermal exploration has been increasing. However, XRD is still the universal standard procedure for doing that analysis. This research determined clay mineral composition through three analysis methods: XRD, IRS, and IRIS. IRS is applied since it has proven its ability to characterise clay mineral types using the ratio between aluminium hydroxyl and water absorption features (Simpson et al., 2013; Simpson & Rae, 2018). With the development of IRIS (i.e., imaging IRS), the tool produces a spectrum for every image pixel. Thus, IRIS has more spectra which likely can detect more minerals than non-imaging IRS. IRIS assigns pixels into minerals based on their (dominant) spectral features (Savitri et al., 2021). The resulted mineral maps can also be used to semi-quantify the mineral composition of the samples based on the minerals' areal percentage.

Correa et al. (2013) have compared the clay composition to MeB and resistivity values, but they only used mainly IRS combined with XRD on selected samples. In this paper, we integrate the clay identification results from the three analytical methods to better understand how the clay composition variation may influence the variation of MeB and resistivity values and how this may change our knowledge about the location of the geothermal reservoir. This research is built on Rantau Dedap geothermal system (Fig. 1) using samples from two drilling wells.

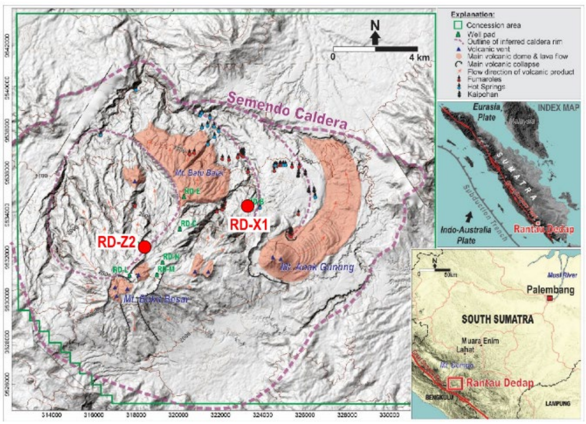

Figure 1: Location of the study area (from Mussofan et al. (2021)). This research uses samples from two drilling wells (RD-X1 and RD-Z2) as indicated in the map.

2. GEOLOGICAL FRAMEWORK

Rantau Dedap geothermal system occurs in a back-arc basin of the Indo-Australian – Eurasian Subduction Zone. The occurrence and structure of the system are controlled by the NW-SE dextral strike-slip Great Sumatran Fault (GSF) and the reactivation of the NE-SW basement structure; both were products of the subduction (Sidik et al., 2018).

The stratigraphy of the area consists of Tertiary volcanic products with a composition of silicic to dacitic. A mixed sediment and tuff unit is intercalated with these volcanic products (Mussofan et al., 2021; Sidik et al., 2018). The Subaqueous Debris Flow unit, having a wide variety of rock fragments from volcanic to limestone to mudstone, overlies these silicic volcanic products. These entire sequences were presumed to be a caldera-fill product (Mussofan et al., 2021). Subaerial Dacite to Andesite overlies the Subaqueous Debris Flow. At the top, the lithology is dominated by andesitic volcanic products from Bukit Besar Andesite and other young volcanic units (Mussofan et al., 2021).

Several works have been done to understand the permeability structure of the Rantau Dedap geothermal system. Dyaksa et al. (2016) showed a poor relationship between the decrease of MT resistivity value with the top of reservoir permeability. The smectite clay alteration zone appears to be ~600 m shallower than the top of reservoir permeability from the resistivity value. It is presumed that this gap was due to a mixed-layer clay zone having a moderate to high resistivity. Later work described that the permeability of the Rantau Dedap geothermal system is strongly controlled by stratigraphy (Mussofan et al., 2019).

3. CLAY MINERALS COMPOSITION

3.1 Composition of clay-fraction samples

The XRD and IRS analyses produce a descriptive composition of the clay-fraction samples (Fig. 2, Fig.3). Both methods generally show similar results, with IRS appearing to be slightly more sensitive in detection limits. IRS can detect smectite (or traces of it) in some samples where XRD does not. The use of glycolation treatment on the IRS samples increased the confidence level of the smectite identification because smectite will have several additional absorption features on the glycolated samples. One additional feature that is always visible in the glycolated sample spectra is the feature at 2280nm. The shift of this feature to a shorter wavelength position is thought to represent the decrease of the smectite content. The glycolation treatment on IRS samples still cannot differentiate whether smectite and illite occur as interlayered minerals or as two separate minerals, unlike XRD.

According to IRS, there are two samples of RD-Z2 that has kandite minerals, but XRD cannot detect them. However, XRD detects smectite-illite interlayered clay in these samples. Nonetheless, only the spectral properties of smectite & chlorite are apparent in IRS, while the kandites absorption features have obscured the spectral properties of illite. No interlayered smectite-chlorite is found in the samples.

3.2 Composition and (semi-)quantitative interpretation of clay minerals in the cuttings

Clay mineral identification using IRIS method was made using a "decision-tree" classification algorithm built for all the main geothermal index minerals developed by Savitri et al. (2022). The analysis was done on the original cuttings, and, thus, the percentage bars in Fig.2 and Fig.3 show the (semi-)quantification of the clay minerals in the whole rock. The length of this bar represents the number of clay minerals classified in the entire cuttings. As the spectrum from each pixel was a function of all minerals present in that pixel, IRIS can only detect if several minerals occur in one pixel without being able to differentiate whether those were interlayered clays or different clay minerals that occur spatially close one to another. Therefore, we use the term "mixture" in the IRIS results.

The results show a more visible correlation with XRD and IRS results on RD-X1 samples (Fig. 2). The identification of smectite, illite, and chlorite indicates an agreement between the three methods. The more classified pixels the mineral has in IRIS, the higher the posibility for it to be detected by XRD and IRS. At ~525m depth, IRIS detected only a small number of smectite pixels. As predicted, it only show traces of absorption features in IRS and even remains undetected by XRD.

The RD-Z2 well does not have many samples with more than 5% smectite classified from IRIS (Fig. 3). Consequently, they are hardly to be seen in the clay percentage bars. However, the similarity of identification results between the three methods is clear for illite and chlorite. Kandite minerals occupy >40% of samples at ~730m depth. It is also detected by IRS, but absent in XRD despite of the exact same samples being used. It further confirms that infrared spectroscopy (both IRS and IRIS) is more sensitive in identifying kandite minerals.

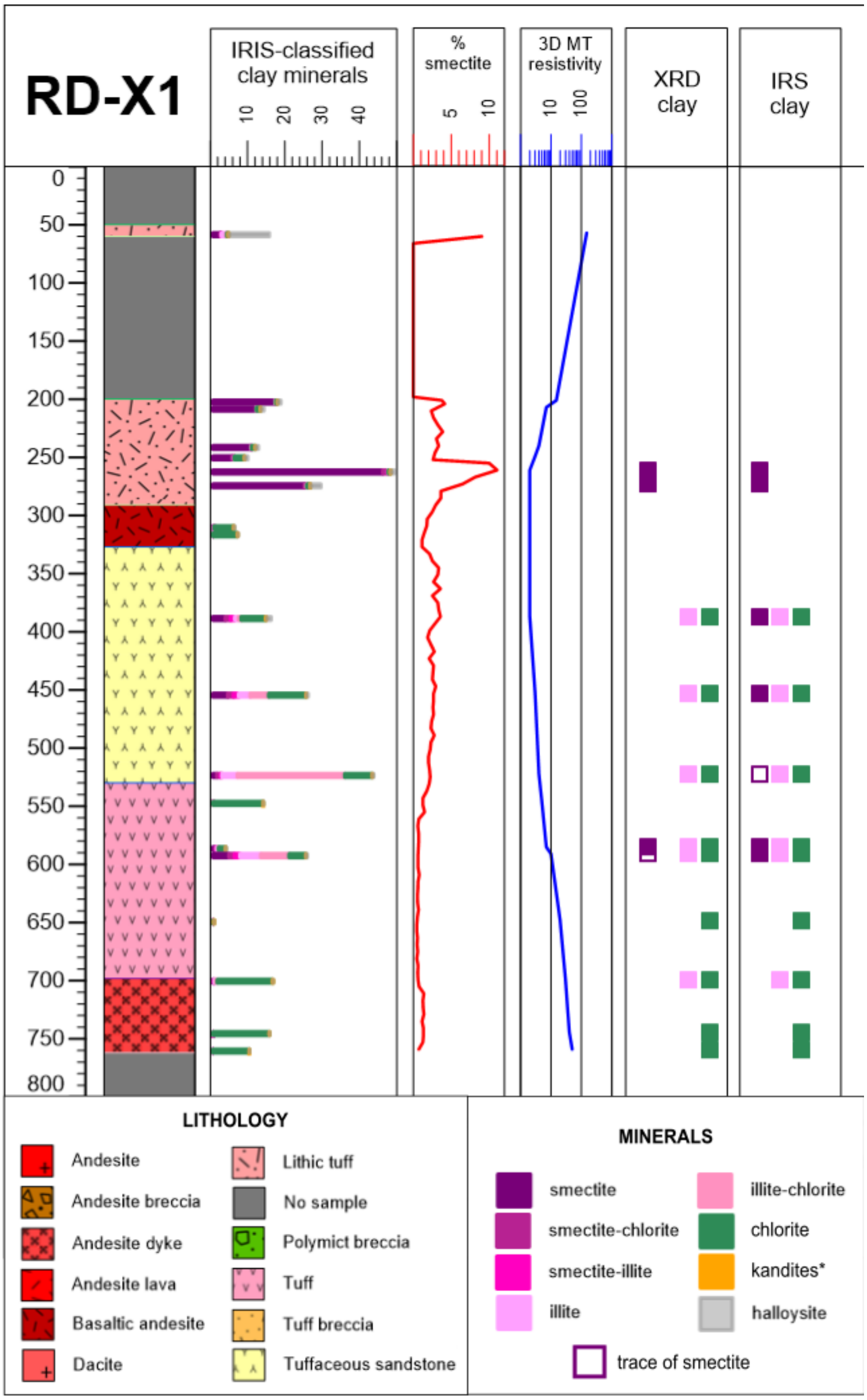

Figure 2: The comparison between lithology, clay minerals identification obtained using the three analyses methods, % smectite calculated from MeB stain test results, and 3D MT resistivity value for RD-X1 well. For the IRIS identification results, halloysite is coded with different colour and not included in the kandite minerals as most of the halloysite pixels are mixture between one of the kandite mineral and either smectite or illite.

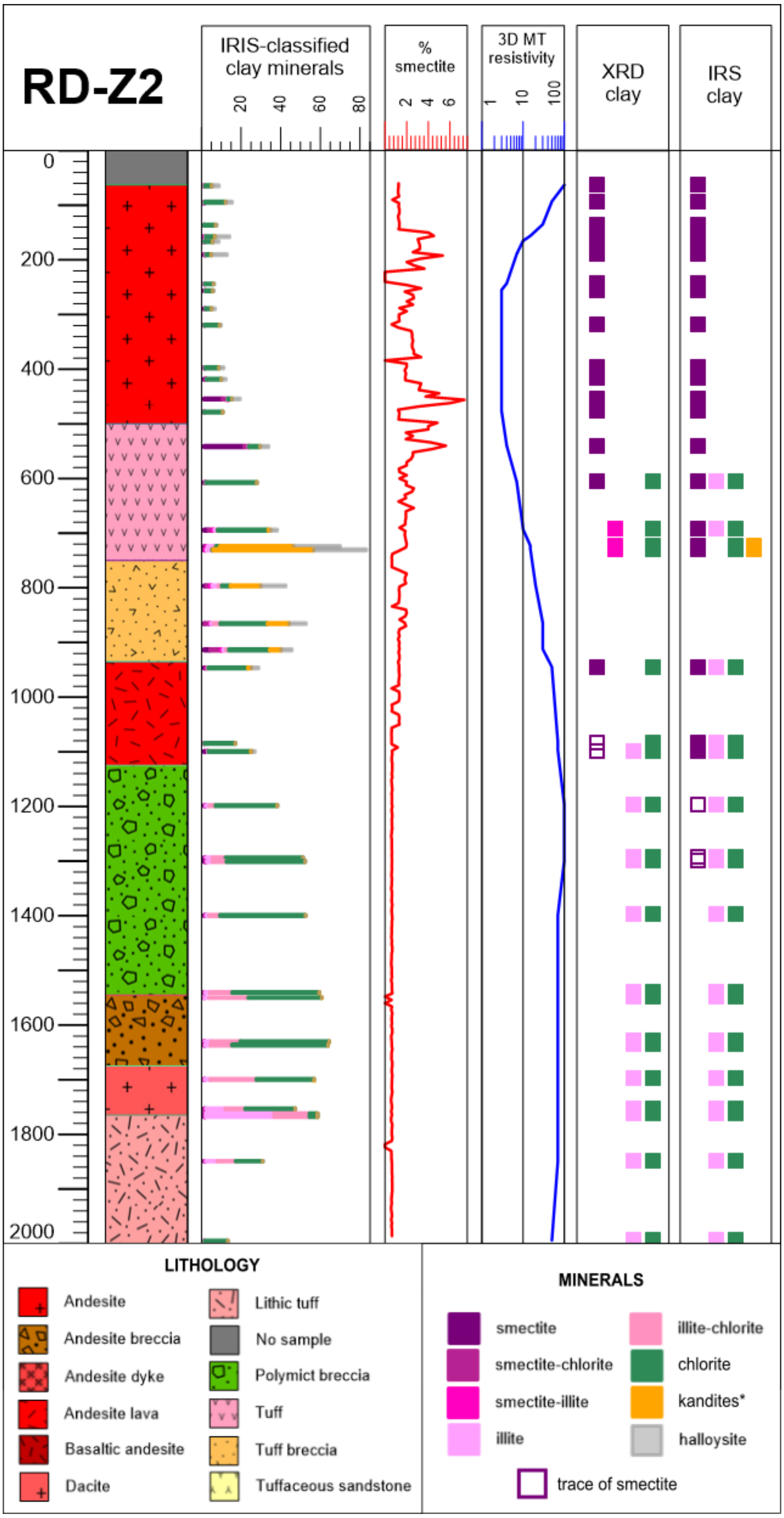

Figure 3: The comparison between lithology, clay minerals identification obtained using the three analyses methods, % smectite calculated from MeB stain test results, and 3D MT resistivity value for RD-Z2 well. For the IRIS identification results, halloysite is coded with different colour and not included in the kandite minerals as most of the halloysite pixels are mixture between one of the kandite mineral and either smectite or illite.

4. COMPARISON TO DRILLING DATA

4.1 Methylene Blue (MeB) stain test results

MeB stain test is the first scanning tool applied at geothermal drilling sites to indicate the smectite content in the sample. The amount (in mL) of MeB dye needed to change the colour of the rock solution is used to calculate the Cation Exchange Capacity (CEC) of the MeB (Topal, 1996; Yukselen & Kaya, 2008). Smectite has a CEC range 80-150 meq/100g (miliequivalent/100 gram), but in this research we assume that the CEC of smectite is 100 meq/100g. Therefore, every 1 meq/100g CEC MeB is equivalent to 1% of smectite in the sample.

The comparison shows that MeB results indicate a higher "%smectite" in the samples where XRD and IRS identify only smectite. When the sample contains smectite but other clay mineral is also present, the "%smectite" decreases. In RD-X1 at ~600 m depth, the three methods identified smectite, but the MeB results did not indicate them. This suggests that MeB may have some detection limit for the mineral. From XRD and IRS results, smectite is absent at depth greater than 650m in RD-X1 and 1400m in RD-Z2. At these depths, the MeB test results show a flat line with a minimum "%smectite" value. However, the CEC of MeB does not drop to zero because there is still a minor response to MeB by other clay minerals or other high cation exchange minerals (Gunderson et al., 2000). As there is only 2 samples having interlayered smectite-illite, the correlation between this type of clay and MeB results remains uncertain.

Correa et al. (2013) found that in Wairakei Geothermal Field (New Zealand), the decrease of MeB values reflects the decrease of smectite content rather than the transition from smecite to illite. Our comparison also show a similar relationships, and also vice versa. In RD-X1, IRS detects smectite at depth 380-520 m) and IRIS suggest that illite dominates the clay composition although smectite is present. However, the MeB results show a similar value to the shallower depth where illite is absent.

We did a multiple regression analysis using the areal percentage of smectite-related classes identified by IRIS (i.e., smectite, smectite-chlorite, and smectite-illite mixtures) to find out which one of the three minerals that has the strongest effect on the variation of MeB test results. The calculation shows that smectite has the strongest influence, indicated by the highest gradient of the regression line (Fig. 4). Following smectite, smectite-chlorite mixture has a stronger influence towards the variation of MeB value compared to smectite-illite.

Sample number 1, 23, 25, and 32 (i.e., RD-X1/57-60m, RD-Z2/156-159m, RD-Z2/189-192m, and RD-Z2/453-456m, respectively) appear as outliers in the smectite-MeB regression relationships, where IRIS classified less smectite compared to what is indicated by the MeB results (Fig. 4A). It is because these samples contain abundant kandite minerals which occur spatially close to the smectite. The mixture between smectite and kandite mineral produce combined spectra that look similar to the spectra of halloysite. Hence, many smectite minerals were classified as halloysite class.

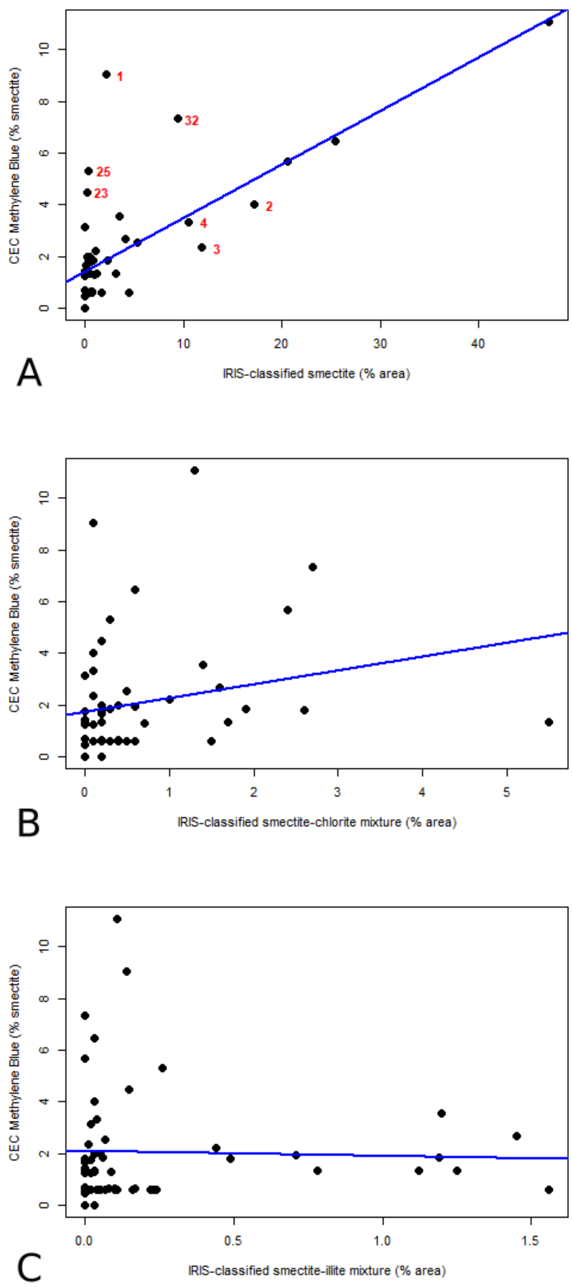

Figure 4: Scatter plots illustrating the effect of each IRIS smectite-related class on the MeB stain test results: (A) smectite class; (B) smectite-chlorite class; and (C) smectite-illite mixture class.

Sample number 2, 3, 4 also appear as outliers (i.e., RD-X1/201-204m, RD-X1/207-210m, and RD-X1/240-243m, respectively). On the contrary, these samples seem to have more smectite classified by IRIS than indicated by MeB result. It is related to the lithology of which fragments of volcanic glass are present in the cuttings. These rock fragments has spectral properties that look similar to smectite so that they were also classified as smectite by IRIS.

4.2 3-dimensional MT resistivity value

The scatter plots between each clay mineral class and MT resistivity values (Fig. 5 and Fig.6) indicate that the type of clay influences the variation of MT resistivity value more than the amount of the clay itself. Regardless of the (areal) percentage, samples with smectite class have an MT resistivity value under 10 Ωm. Kandites have a higher MT resistivity range, namely 10-40 Ωm. Illite and chlorite indicates a higher MT resistivity range. Samples having these two classes show an MT resistivity value of maximum 100 Ωm, but most of them show a value of 70 Ωm. Any mixture classes with illite (i.e., smectite-chlorite and smectite-illite) have a resistivity value of mostly under 30 Ωm (Fig. 6).

However, the relationships between type of clay components and MT resistivity value is weaker from the XRD and IRS results (Fig. 2 and Fig. 3). In RD-X1, the bottom limit of 10 Ωm resistivity coincides with the deepest occurrence of smectite. Thus, although other clay may be present as well, the resistivity value is still under 10 Ωm as long as smectite is present. On the other hand, this low MT resistivity value in RD-Z2 was only persisted when XRD and IRS detect smectite as the only clay component. Moreover, rocks with the highest MT resistivity value still contain smectite, or at least traces of smectite. If XRD and IRS indicates only illite and chlorite in the sample, the MT resistivity value increased to higher than 50 Ωm. It is applied for both wells.

Although also seen in RD-X1, RD-Z2 samples show strong correlations between lithology and MT resistivity variation (Fig. 3). Low values correlates to tuff and tuffaceous rocks, while high resistivity values occur in breccia and dacite (Fig. 7). The andesite of RD-Z2 and basaltic andesite of RD-X1 shows a significantly low resistivity value compared to the amount of smectite (and halloysite class) indicated by IRIS results. The conductive property of these rocks is likely due to the presence of hydrothermal fluid suggesting that the rocks are intensively fractured.

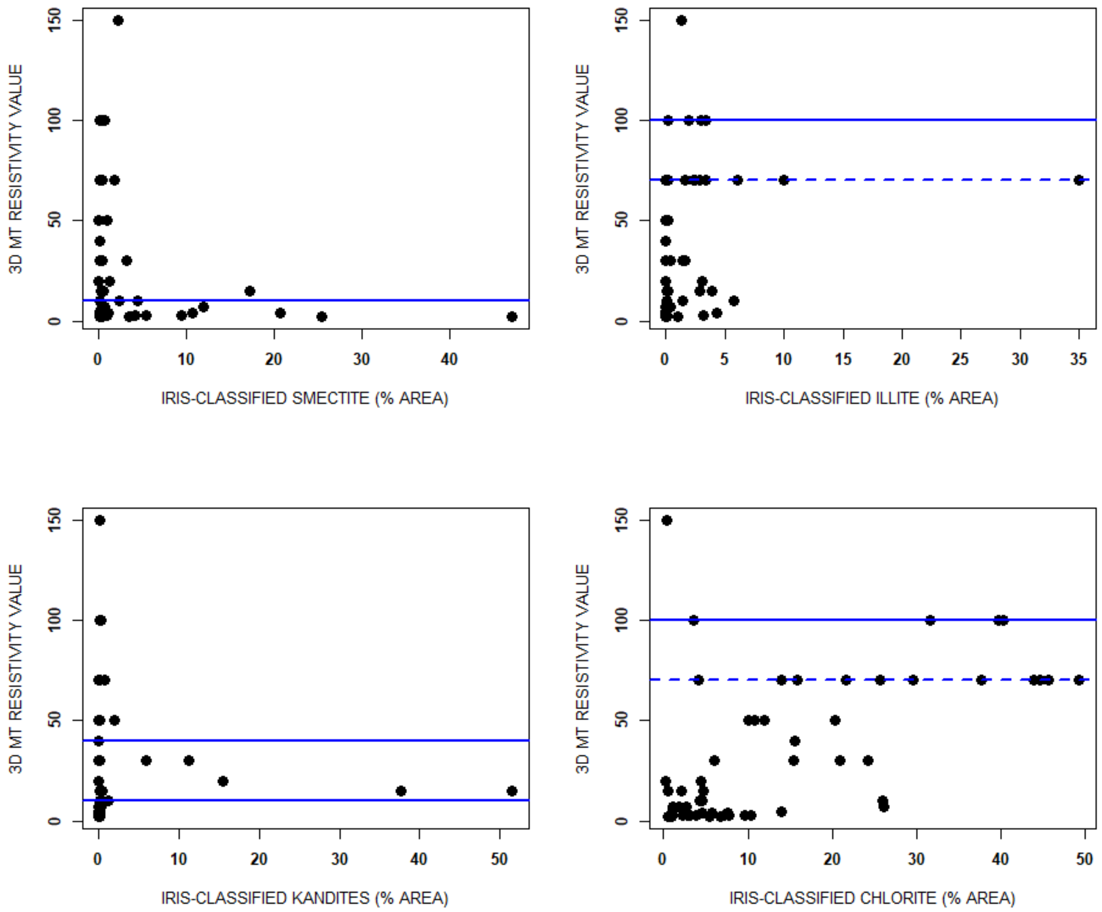

Figure 5: Scatter plots showing the correlation between each IRIS clay mineral class and 3D MT resistivity value.

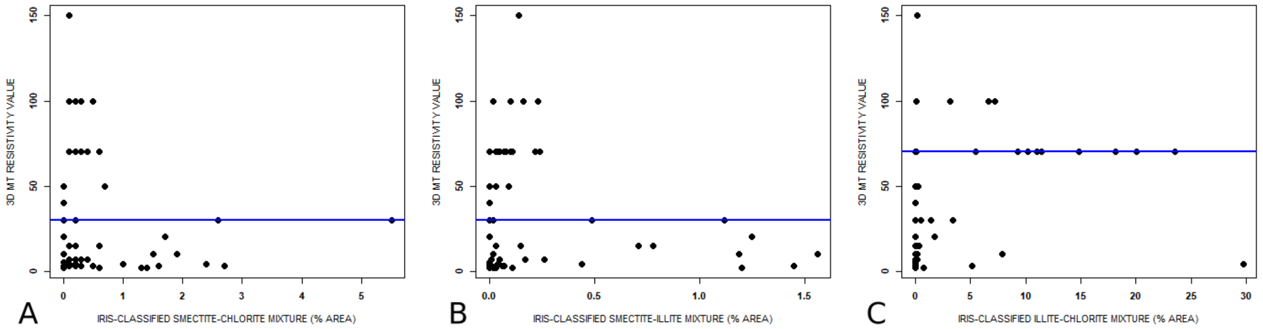

Figure 6: Scatter plots showing the correlation between each IRIS clay mineral mixture class and 3D MT resistivity value: (A) smectite-chlorite mixture; (B) smectite-illite mixture; and (C) illite-chlorite mixture.

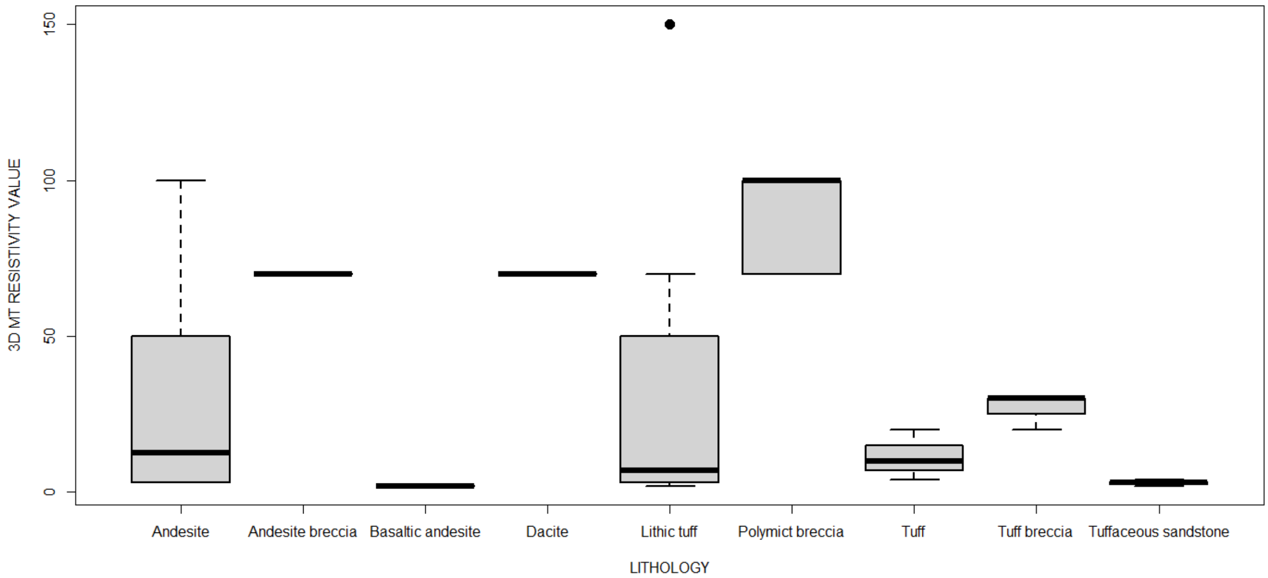

Figure 7: Relationships between each lithology and 3D MT resistivity value. Andesite includes andesite, andesite dyke, and andesite lava units in Figure2 and Figure 3.

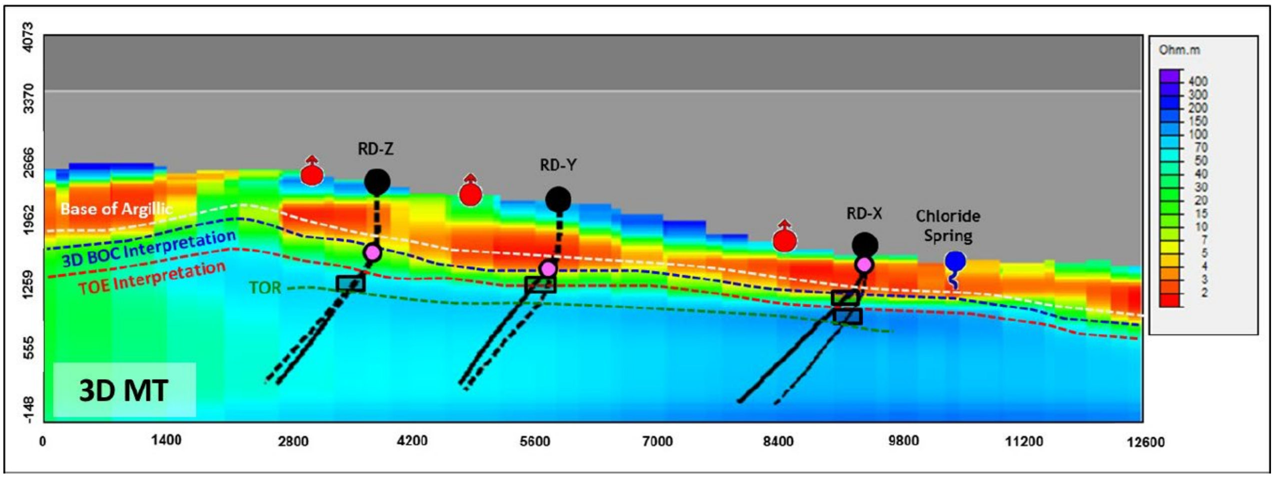

Figure 8: The cross section of Rantau dedap 3D inversion MT resistivity value (Dyaksa et al., 2016) showing the gap between the base of smectite-rich zone and the top of reservoir.

5. IMPLICATION ON THE UNDERSTANDING OF THE LOCATION OF GEOTHERMAL SYSTEM RESERVOIR

The clay cap, which is a smectite-rich zone, has been identified using a high "%smectite" indicated by MeB test and low resistivity value. This relationship is weaker in our RD-Z2 results. In this well, MeB and MT results suggest a clay cap from 200-550 m depth. XRD and IRS detect smectite as the only clay mineral, but our IRIS analysis indicates that smectite only occurs in a small amount in the upper half of this depth range. In the bottom half of this range (i.e., 400-550 m depth, smectite occupies 20-30 % of samples according to IRIS, which coincides with a "%smectite" of MeB greater than 4. Thus, although the location is in accordance with what the drilling data indicates, the clay cap's thickness may be thinner than suggested.

Below this depth down to 950m depth, there is an intermediate resistivity zone (i.e., 5-50 Ωm) where IRIS indicated smectite-illite, smectite-chlorite mixtures, and kandite minerals. Likewise, XRD and IRS detected smectite, interlayered smectite-illite, and kandites in this zone. Dyaksa et al. (2016) showed that there is a gap between the base of smectite-rich zone and the top of reservoir (Fig. 8) which was thought to be a zone rich in interlayered clay minerals. This matches our findings.

6. CONCLUSIONS

Clay analysis using XRD and IRS produces similar results, especially for smectite, illite, and chlorite. However, the sensitivity of IRS is slightly higher. The identification of smectite-illite interlayered by XRD corresponds to the identification of smectite-illite mixture by IRS. In the tested clay fraction samples, kandites can only be identified by IRS.

Three smectite-related classes were detected from IRIS: smectite, smectite-chlorite, and smectite-illite mixtures. Among these classes, smectite class has the most influence on the MeB stain test results, followed by smectite-chlorite and smectite-illite mixture class. Samples with a significant amount of smectite classified by IRIS are those having greater than 4% smectite according to MeB test. Different types of clay correlate to different MT resistivity value. Smectite correlates to below 10 Ωm, kandite minerals correlate to 10-40 Ωm, while illite and chlorite mainly correlate to 70 Ωm. A mixture between smectite and either illite or chlorite correlates to a low to intermediate resistivity value of up to 30 Ωm. In addition to clay mineral types, lithology also significantly influences the variation of resistivity values. It is likely that the top of reservoir in our geothermal system is located at the zone where smectite and kandite minerals are absent, namely at resistivity value greater than 50 Ωm.

REFERENCES

Correa, N. A. A., Rae, A. J. A., & Sepulveda, F.: Distribution of clay minerals through a conductive (MT) zone on the margins of a high-temperature geothermal reservoir, Wairakei Geothermal Field, Taupo Volcanic Zone, New Zealand, *Transactions - Geothermal Resources Council*, *37*, (2013), 459–462.

Dyaksa, D., Ramadhan, I., & Ganefianto, N.: Magnetotelluric Reliability for Exploration Drilling Stage: Study Cases in Muara Laboh and Rantau Dedap Geothermal Project, Sumatera, Indonesia, *Proceedings of the 41st Workshop on Geothermal Reservoir Engineering*, Stanford, California, (2016).

Gunderson, R., Cumming, W., Astra, D., & Harvey, C.: Analysis of smectite clays in geothermal drill cuttings by the methylene blue method: for well site geothermometry and resistivity sounding correlation, *Proceedings World Geothermal Congress 2000*, Kyushu - Tohoku, Japan, (2000), 1175–1181.

Mussofan, W., Baroek, M., Stimac, J., Santana, S., Ganefianto, N., Ramadhan, I., Sidik, R. P., & Dyaksa, D. A.: Rantau Dedap Geology and Alteration Update, *Proceedings 46th Workshop on Geothermal Reservoir Engineering*, Stanford, California, (2021).

Mussofan, W., Stimac, J., Baroek, M. C., Colvin, A., Sidik, R. P., & Ganefianto, N.: Thick Silicic Volcanic Sequences At Muara Laboh and Rantau Dedap Geothermal Fields, Sumatra, Indonesia: Implications for Reservoir Architecture and Permeability, *Proceedings 41st New Zealand Geothermal Workshop*, Auckland, New Zealand, (2019).

Rosenberg, M. D.: Smectite clay content in rock and soil material: A Method for Quantitative Estimation by Methylene Blue Dye Absorption, *GNS Science Letter Report (Non-Confidential) LR2008/316LR*, (2008), 4.

Savitri, K. P., Hecker, C., van der Meer, F. D., & Sidik, R. P.: VNIR-SWIR infrared (imaging) spectroscopy for geothermal exploration: Current status and future directions, *Geothermics*, *96*, (2021).

Savitri, K. P., Hecker, C., van Ruitenbeek, F. J. A., & Sihotang, M. A. H.: A knowledge-based classification of hyperspectral rock images for targetting geothermal index minerals, *Manuscript in Preparation*, (2022).

Sidik, R. P., Mussofan, W., Wallis, I., Azis, H., Stimac, J., & Ganefianto, N.: Two contrasting geothermal fields in Sumatra, Indonesia: Muara Laboh and Rantau Dedap, *Proceedings of the 40th New Zealand Geothermal Workshop*, Taupo, New Zealand, (2018).

Simpson, M. P., & Rae, A. J.: Short-wave infrared (SWIR) reflectance spectrometric characterisation of clays from geothermal systems of the Taupō Volcanic Zone, New Zealand, *Geothermics*, *73*, (2018), 74–90.

Simpson, M. P., Rae, A. J., Ganefianto, N., & Sepulveda, F.: Short wavelength infrared (SWIR) spectral characterisation of smectite, illite-smectite and illite for geothermal fields of the Taupo Volcanic Zone, New Zealand, *Proceedings of the 35th New Zealand Geothermal Workshop*, Rotorua, New Zealand, (2013), 17–20.

Topal, T.: The Use of Methylene Blue Adsorption Test to Assess the Clay Content of the Cappadocian Tuff, *Icomos*, *2*, (1996), 791–799.

Ussher, G., Harvey, C., Johnstone, R., Anderson, E., & Zealand, N.: Understanding the resistivities observed in geothermal systems, *Proceedings World Geothermal Congress 2000*, Kyushu - Tohoku, Japan, (2000), 1915–1920.

Yukselen, Y., & Kaya, A.: Suitability of the methylene blue test for surface area, cation exchange capacity and swell potential determination of clayey soils, *Engineering Geology*, *102*(1–2), (2008), 38–45.

Acknowledgements

This work is collaborative research between the Faculty of Geo-information Science and Earth Observation (ITC), University of Twente and PT Supreme Energy Rantau Dedap (SERD). We thank PT SERD for permitting the publication of this paper. We also thank Thomas Groen for the helpful assistance on the statistical analysis. This work is funded by the Geothermal Capacity Building Programme Indonesia – The Netherlands (GEOCAP) [Reference No.: ESA-075.18/ls].